

The American Journal of Human Genetics, Volume 105

Supplemental Data

Pathogenic Variants in *NUP214*

**Cause “Plugged” Nuclear Pore Channels
and Acute Febrile Encephalopathy**

Boris Fichtman, Tamar Harel, Nitzan Biran, Fadia Zagairy, Carolyn D. Applegate, Yuval Salzberg, Tal Gilboa, Somaya Salah, Avraham Shaag, Natalia Simanovsky, Houriya Ayoubieh, Nara Sobreira, Giuseppe Punzi, Ciro Leonardo Pierri, Ada Hamosh, Orly Elpeleg, Amnon Harel, and Simon Edvardson

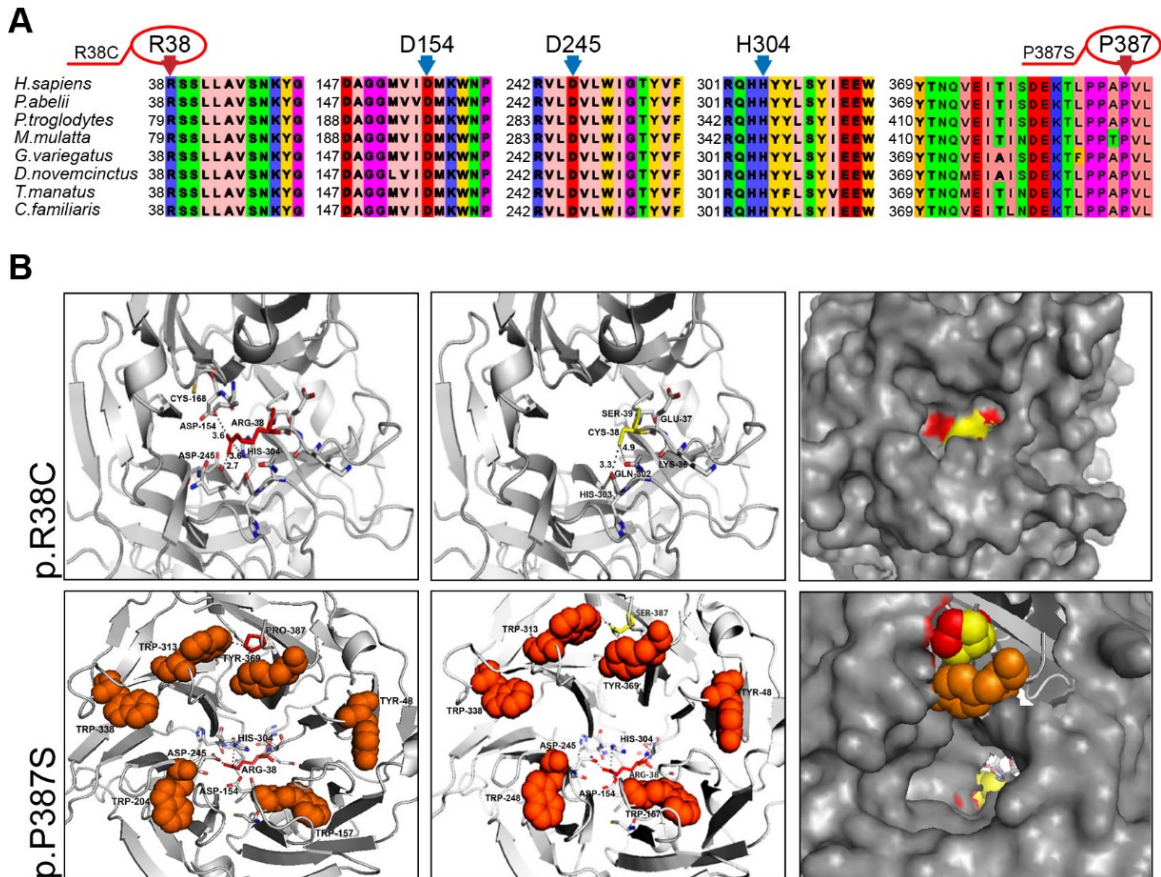


Figure S1. Comparative modelling of the *NUP214* variants in two families.

(A) Select portions of multiple sequence alignment of *NUP214* orthologs sampled through mammalia. The high evolutionary conservation of R38 and P387, and of the residues which directly interact with R38 (i.e., D154, D245, and H304) can be appreciated. (B) 3D comparative models of the R38C (upper panels) and P387S (lower panels) variants. Upper left panel demonstrates a top view of the 3D structure of the *NUP214* N-terminal domain (3fhc.pdb), in grey cartoon representation. Residues within 4 Å from R38 (in red sticks) are reported in white sticks, and are predicted to form an ion network. Upper middle panel demonstrates the 3D comparative model of the *NUP214* R38C mutant. Residues within 4 Å from C38 (in yellow sticks) are reported in white sticks, showing altered interactions as compared to wild type. Upper right panel shows the superimposition of *NUP214* (red surface representation) and *NUP214_R38C* (yellow surface representation) in a grey central pocket. Bottom left panel depicts a bottom view of the 3D structure of the *NUP214* N-terminal domain (3fhc.pdb), in grey cartoon representation. P387 (bottom left panel) and S387 (bottom middle panel) are reported in stick representation, red and yellow, respectively. Black dashed lines between P387 and Y369 and W313 indicate interactions shorter than 3.9 Å. Aromatic residues located on the

surface of NUP214 are reported in orange sphere representation. Bottom right panel shows the superimposition of NUP214 and NUP214_R38C/P387S highlighting the exploded view of R38 (red spheres at the bottom of the cavity) replaced with a cysteine residue (yellow spheres at the bottom of the cavity) and P387 (red spheres at the top of the cavity) with a serine residue (yellow spheres at the top of the cavity), close to Y369 (orange spheres).

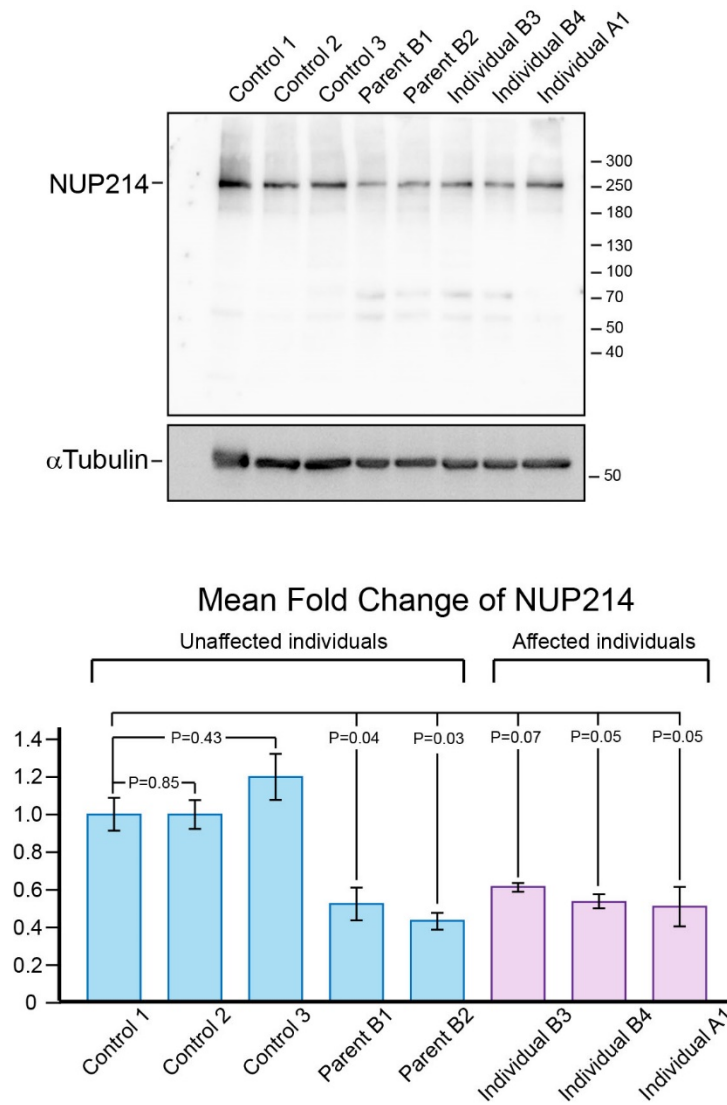


Figure S2. Extended immunoblot analysis of NUP214 levels in fibroblasts from control and affected individuals. Total cell lysates were prepared from primary fibroblast cultures of three unrelated controls, two unaffected parents from Family B, affected individual A1 from Family A and affected individuals B3 and B4 from Family B. Three separate lysates were prepared for each cell line and immunoblots were stained with anti-NUP214 and normalized against α -tubulin. A quantitative analysis of multiple (≥ 3) blots from 3 separate lysates is shown

in the bar chart. Bars indicate SEM. All three affected individuals showed a consistent reduction of NUP214 to ~50% of its level in the three controls. Surprisingly, both of the unaffected parents had similarly low levels of NUP214 in their total cell lysates. It should be noted, however, that each parent has one WT allele encoding a fully functional protein. See Figure 3 for an assessment of NUP214 protein localized to the nuclear envelope.

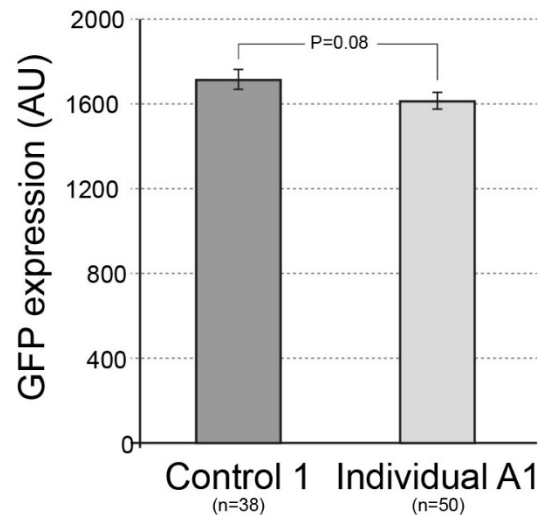


Figure S3. Quantitative comparison of GFP expression levels in control and affected individual-derived cells following transfection. For the analysis of mRNA export in fibroblasts described in Figure 5B it was important to establish that the exogenous GFP construct is expressed in control and affected cells at a comparable level. GFP-expressing cells were randomly chosen in 3 independent experiments. The average staining intensity per cell was measured after delineating cell boundaries in ImageJ, as explained in Materials and Methods. Bars indicate SEM; n = number of cells analyzed.

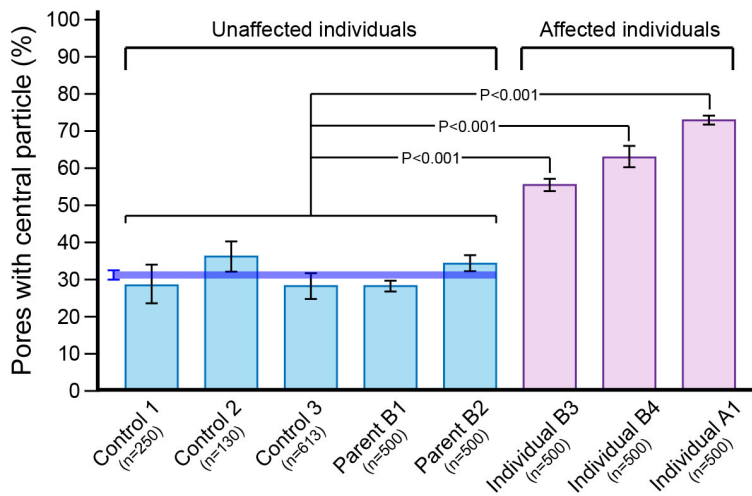
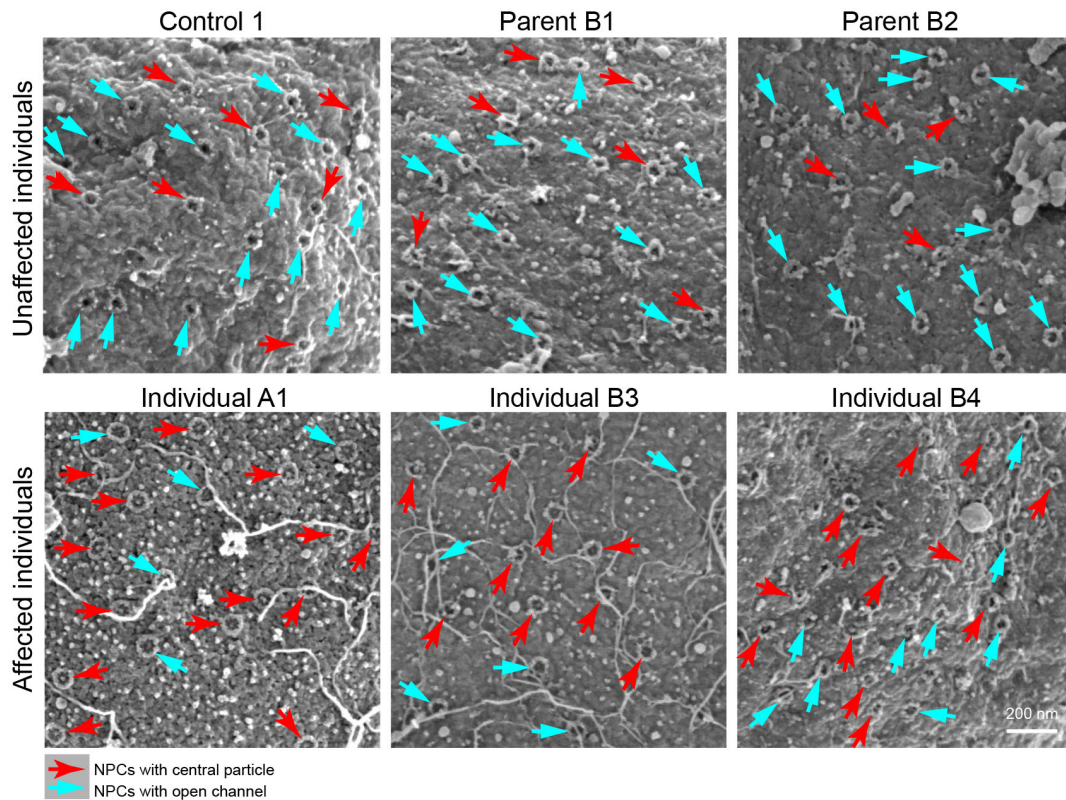


Figure S4. Extended analysis of “central plugs” in NPC channels in unaffected individuals and in affected individuals from families A and B. Direct surface imaging by FESEM was performed, as in Figure 6, on exposed nuclei from primary fibroblast cultures of three unrelated controls, two unaffected parents from Family B, affected individual A1 from Family A and affected individuals B3 and B4 from Family B. Two independent experiments were performed for all the primary fibroblast lines. Representative flat areas of nuclear envelopes with NPCs are shown for three unaffected and three affected individual-derived nuclei. The bar chart summarizes a quantitative analysis of individual NPCs from multiple randomly chosen flat

areas, scored as either having an open central channel or a recognizable central particle. Bars indicate SEM; n = number of NPCs analyzed. Note that each of the affected individual-derived fibroblast lines is characterized by a significantly higher proportion of NPCs with central particles compared to the average of five unaffected individuals.

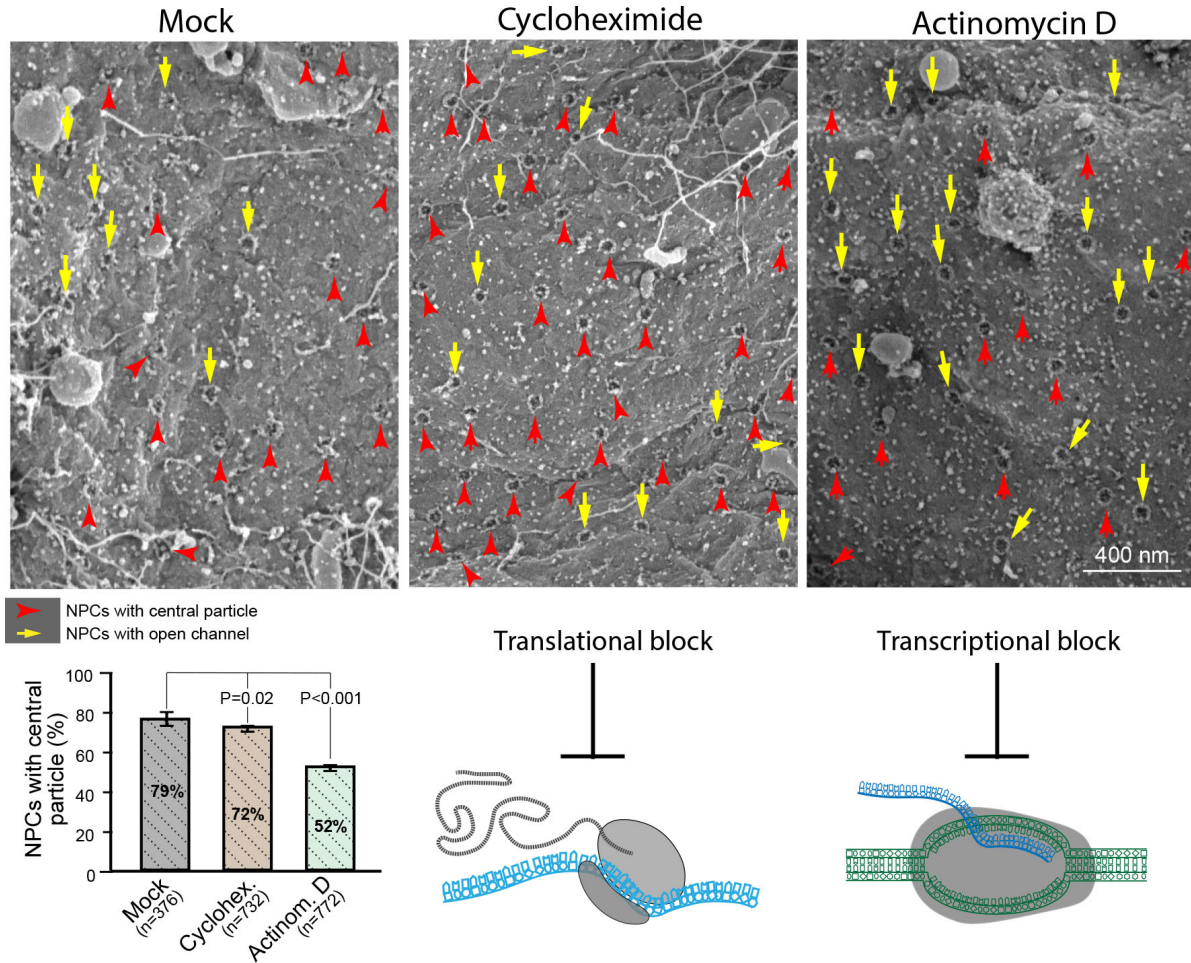


Figure S5. Inhibition of transcription reduces the prevalence of “central plugs” in the NPC channels of affected cells. The effect of pre-treatment with transcription and translation inhibitors on the prevalence of central channel particles was tested in individual A1-derived fibroblasts, that showed the highest proportion of “plugged” NPCs (see Figure S4). Fibroblasts were pre-treated with 5 µg/ml cycloheximide, 1 µg/ml actinomycin D or mock treated (DMSO only) for 24 h and processed for FESEM imaging and quantitative analysis of “central plugs” as in Figures 6 and S4. Representative areas of nuclear envelopes are shown and the bar chart summarizes two independent experiments. Bars indicate SEM; n = number of NPCs analyzed.

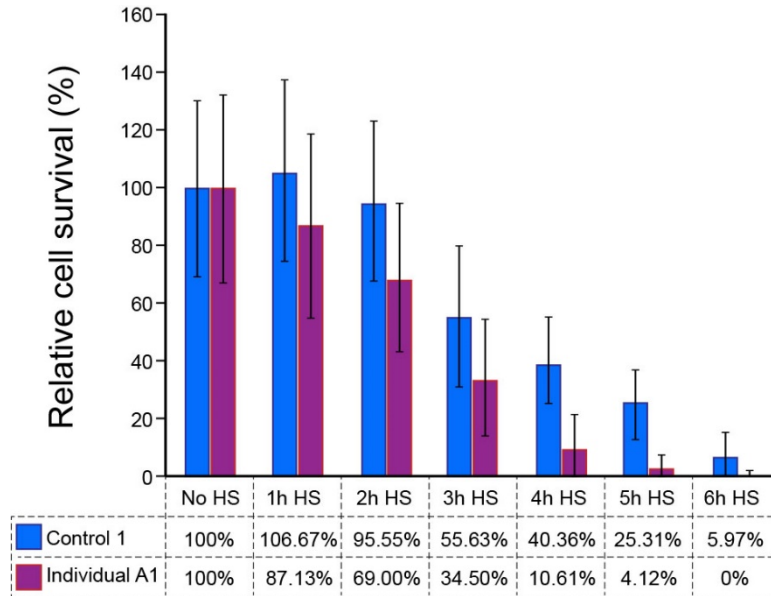


Figure S6. The differential response of primary fibroblasts to the length of time of exposure to heat shock. Control and affected individual-derived primary fibroblasts were grown under identical conditions and then subjected to HS of 43°C for different amounts of time, followed by an immediate determination of cell viability by Trypan blue staining. Bars represent mean \pm S.E.M. for 3 independent experiments.

Table S1. Homozygous rare variants shared by affected individuals in Family A

Gene	Position [hg19]	RefSeq	Nucleotide	Protein	gnomAD	GERP	MutTast
<i>NUP214</i>	Chr9: 134002977C>T	NM_005085.3	c.112C>T	p.Arg38Cys	0.00007	5.74	D
<i>FARP2</i>	Chr2:242343259A>G	NM_014808.3	c.200A>G	p.Gln67Arg	0.000004	3.45	D

Abbreviations: D – disease causing (predicted); MutTast – mutation taster

Table S2. *NUP214* variant interpretation and bioinformatic predictions

Position [hg19]	Nucleotide *	Protein	gnomAD (all)	gnomAD (highest population MAF)	Bravo/Topmed	GERP	CADD	MCAP	MutTast	SIFT	Polyphen	ACMG**
Chr9: 134002977C>T	c.112C>T	p.Arg38Cys	0.000064	0.00011 (European)	-	5.74	33	PoP	D	D	PD	VUS; PP3, PP1
Chr9: 134015962C>T	c.1159C>T	p.Pro387Ser	0.000004	0.0000088 (European)	-	5.76	28.2	PoP	D	D	PD	VUS; PP3, PP1
Chr9: 134019946delC	c.1574delC	p.Pro525Leufs*6	0	0	-	4.72	NR	NR	NR	NR	NR	Likely pathogenic; PM2, PM3, PM4, PP1

*RefSeq NM_005085.3

** Variant interpretation according to ACMG standards and guidelines¹

Abbreviations: D – disease causing (predicted)/d134amaging; MAF – minor allele frequency; MutTast – mutation taster; NR – not relevant; PD – probably damaging; PM2 – pathogenic moderate; PoP – possibly pathogenic; PP3 – pathogenic supporting; VUS – variant of uncertain significance.

Supplemental reference

1. Richards, S., Aziz, N., Bale, S., Bick, D., Das, S., Gastier-Foster, J., Grody, W.W., Hegde, M., Lyon, E., Spector, E., et al. (2015). Standards and guidelines for the interpretation of sequence variants: a joint consensus recommendation of the American College of Medical Genetics and Genomics and the Association for Molecular Pathology. *Genet Med* 17, 405-424.